




## PAPER

[View Article Online](#)  
[View Journal](#) | [View Issue](#)Cite this: *RSC Sustainability*, 2025, 3, 275

## Environmental and life cycle assessment of lithium carbonate production from Chilean Atacama brines†

Zijing He,<sup>a</sup> Anna Korre,<sup>b</sup>  <sup>\*ab</sup> Geoff Kelsall,<sup>c</sup> Zhenggang Nie  <sup>a</sup> and Melanie Colet Lagrille  <sup>d</sup>

The exponentially growing market for lithium-ion batteries (LIBs) is driving the development of more environmentally benign processes for producing lithium carbonate, a key precursor. Extracting lithium(I) from brine is a cost-effective method, particularly in the Lithium Triangle in South America, including the Atacama Desert in Chile. Life cycle assessment (LCA) was used to assess the environmental impacts of lithium(I) production by establishing a comprehensive life cycle inventory (LCI) with data from modelling, literature, technical reports and the Ecoinvent database. Information about evaporation rates from Atacama salars, the performance of the northern Chile electrical grid fuel mix and present waste management processes were analysed to establish the water balance, water footprint (WF), water scarcity footprint (WSF) and to estimate in Aspen Plus and Sphera the environmental performance of the battery-grade lithium carbonate production process. The results predicted significant environmental impacts associated with production of input chemicals such as sodium hydroxide (NaOH) and sodium carbonate (Na<sub>2</sub>CO<sub>3</sub>), as well as with energy conversion from the carbon intensive electrical supply in northern Chile. The waste dumps and surface impoundments required for the production process did not result in significant leachate infiltration, although considerable land areas are occupied. The modelling and analysis results highlighted the importance of accurate brine evaporation rates on the process water balance estimation and on the conventional manufacturing process emissions; insufficient evaporation rates increased the water footprint of chemical production processes. The water resource stress in the arid Atacama region was evident from predicted water balances, WFs and WSFs, emphasising the necessity to innovate less time-consuming and water-conserving processes to increase sustainability.

Received 7th May 2024  
Accepted 8th November 2024

DOI: 10.1039/d4su00223g

[rsc.li/rscsus](https://rsc.li/rscsus)

## Sustainability spotlight

The global necessity to decarbonise energy storage and conversion systems is causing rapidly growing demand for lithium-ion batteries, so requiring sustainable processes for lithium carbonate (Li<sub>2</sub>CO<sub>3</sub>) production. We established a comprehensive life cycle inventory to evaluate environmental impacts of its production by evaporation of Atacama brines, analysing effects of brine composition, water supply, evaporation rates, waste management and chemical processes deployed. Results highlight significant environmental and water resource impacts, emphasising the urgency of transitioning to water-saving and more energy efficient processes in arid regions and the importance of site-specific information for accurate emissions and environmental impacts assessment. Identifying and evaluating the impacts of Li<sub>2</sub>CO<sub>3</sub> production is essential for developing materials utilisation strategies aligned with United Nations sustainable development goals (SDG 6, 7, 9, 13 and 15).

## 1 Introduction

Demand for lithium(I) compounds is growing rapidly, driven by the global necessity to decarbonise chemical-to-electrical energy conversion with renewable energy systems, addressing their intermittency and balancing electrical power supply and demand by energy storage, *inter alia* in lithium batteries. Fig. 1 shows the global lithium(I) consumption and the proportion of its use in batteries, with global lithium(I) consumption reaching 180 kt a<sup>-1</sup> in 2023.<sup>1</sup> Although affected by the global COVID-19

<sup>a</sup>Department of Earth Science and Engineering, Imperial College London, Exhibition Road, SW7 2AZ, London, UK. E-mail: [zijing.he21@imperial.ac.uk](mailto:zijing.he21@imperial.ac.uk); [a.korre@imperial.ac.uk](mailto:a.korre@imperial.ac.uk)<sup>b</sup>Energy Futures Lab, Imperial College London, Exhibition Road, SW7 2AZ, London, UK<sup>c</sup>Department of Chemical Engineering, Imperial College London, Exhibition Road, SW7 2AZ, London, UK<sup>d</sup>Department of Chemical Engineering, University of Chile, Av. Beauchef 851, 8370458 Santiago, Región Metropolitana, Chile† Electronic supplementary information (ESI) available. See DOI: <https://doi.org/10.1039/d4su00223g>

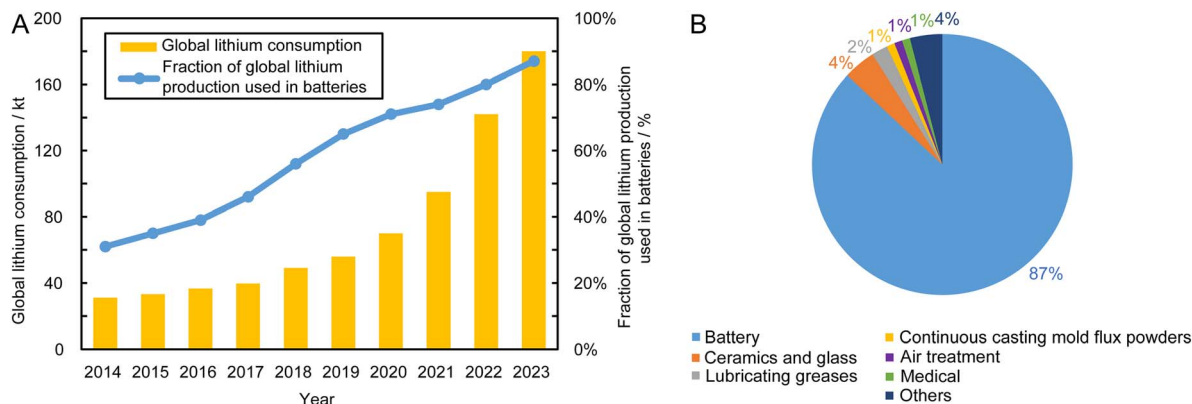


Fig. 1 (A) Global lithium(i) consumption and proportion used in batteries over the last decade. (B) Relative consumptions of lithium(i) in different applications in 2023.<sup>1</sup>

pandemic, demand decreased in the first half year of 2020, but the lithium-ion battery market recovered its strong growth in the second half year, as the global economy started to recover. Between 2020 and 2022, lithium(i) mining output expanded by ca. 80%, despite which market demand for lithium(i) remains tight, resulting in the lithium(i) market price increasing more than five-fold over this period.<sup>2</sup> However, annual average U.S. lithium carbonate prices in 2023 decreased by 32% from those in 2022, mainly due to policy issues, especially relations with China, and slower growth in demand.<sup>1,3</sup> The instability of the lithium(i) market has emphasised the significance of cost-effective, dependable and robust supply chains, particularly for countries that prioritise affordability and those undergoing rapid energy transitions. Lithium(i) can be extracted primarily from hard-rock ores, such as spodumene, petalite and lepidolite, and brines. Australia is the world's leading producer of lithium(i), relying primarily on spodumene, whereas Chile is the second largest producer country, relying on Li<sup>+</sup>-rich brine resources found in high altitude desert salars.<sup>4,5</sup> Interestingly, lithium(i)-containing brines are concentrated mostly in the so-called Lithium Triangle of South America.<sup>6</sup> Extracting lithium(i) from hard rock ores requires various processes, which are complex, energy-intensive and may include several chemical transformations. Due to lower production costs, brine is a more common source of lithium(i), which in principle may be extracted from salt lake brines, geothermal brines and even seawater. However, lithium(i) extraction from geothermal brine has not been commercialised on a large scale, being only at the pre-commercial demonstration stage.<sup>2</sup> As yet, there are no cost-effective processes to extract lithium(i) from seawater, typically at concentrations of 0.1–0.2 ppm,<sup>7,8</sup> whereas lithium(i) concentrations of 200–700 ppm in most salt lake brines are considered as commercially attractive.<sup>9</sup>

Amongst industrial effluents, the formation water produced during oil and gas extraction activities can be considered a potential lithium(i) source, although such brines are typically regarded as waste and are reinjected into the subsurface for disposal.<sup>10</sup> In these brines, lithium(i) concentrations generally range between 1 and 40 mg dm<sup>-3</sup> and depend on the geology of the field.<sup>11</sup> While lithium(i) concentrations in seawater are

typically 0.1–0.2 mg dm<sup>-3</sup>, as mentioned above, brines from reverse osmosis processes used to desalinate seawater contain Li<sup>+</sup> concentrations up to 4 mg dm<sup>-3</sup>, so are more promising potential Li<sup>+</sup> sources compared to seawater.<sup>12</sup> Industrial wastewaters, e.g. from cobalt or nickel recovery processes of lithium-ion battery recycling, can contain up to 3 g Li<sup>+</sup> dm<sup>-3</sup>.<sup>13–15</sup> Recovery of lithium(i) from such resources could enable the industry to develop a circular economy and a strategy to enhance the sustainability of the lithium(i) value chain. Nevertheless, high specific energy consumptions, high costs, Li<sup>+</sup> selectivities against other cations present and slow process kinetics remain significant challenges, requiring further R&D to increase and optimise Li<sup>+</sup> recoveries from industrial effluents.

Lithium(i) concentrations in the South American Atacama desert brines reach 1500 ppm.<sup>16</sup> Salt lake brines are thought to contain over 70% of exploitable lithium(i) resources globally,<sup>1</sup> and about 85% of lithium(i) products are obtained from brines.<sup>17,18</sup> However, salt lake brines have extremely complex compositions, with Na<sup>+</sup> constituting the greatest proportion of cations, including K<sup>+</sup>, Mg<sup>2+</sup> and Ca<sup>2+</sup>, with Cl<sup>-</sup>, CO<sub>3</sub><sup>2-</sup>, SO<sub>4</sub><sup>2-</sup> and borate anions.<sup>19</sup> This causes a significant challenge for purification and selective lithium(i) extraction by various processes being developed, in addition to evaporation technology, as described in the following section. Adsorption by ion exchange of Li<sup>+</sup> ions from brine on e.g. manganese oxides, titanium dioxide, or alumina, can achieve selective recovery when saturated adsorbents in columns are washed with fresh water or acidic solutions, producing lithium(i)-containing solutions. After a specific Li<sup>+</sup> concentration is achieved, sodium carbonate is added to precipitate Li<sub>2</sub>CO<sub>3</sub>.<sup>17,20</sup> Alternatively, liquid–liquid extraction by various organic solvents can be used to extract LiCl selectively.<sup>20,21</sup> Such solvents include β-diketones, *n*-butanol, neutral organophosphorus compounds, and kerosene.<sup>21,22</sup> Although these solvents can differentiate effectively LiCl from NaCl and KCl, separating LiCl from MgCl<sub>2</sub> is more difficult. Increasing selectivity between Li<sup>+</sup> and Mg<sup>2+</sup> often necessitates significant adjustments to pH or brine composition, requiring large amounts of chemicals. Solar evaporative processes predominate in Chile, because of their low costs and as the sensitivity of the environment in the Chilean Atacama



region, where water is extremely scarce, precludes processes that require large freshwater inputs to resolve pollution issues.

Common forms of lithium salts include lithium chloride (LiCl), lithium hydroxide (LiOH), and lithium carbonate ( $\text{Li}_2\text{CO}_3$ ). LiCl can be sourced from lithium-rich hard rock resources, salt lake brines, geothermal brines, and from lithium battery recycling. Although LiCl is not directly useable in LIBs, it is a valuable intermediate for converting to LiOH or  $\text{Li}_2\text{CO}_3$ ; the latter, a primary compound for LIB production, can be produced by reacting LiCl with  $\text{Na}_2\text{CO}_3$ .<sup>23</sup> LiOH, another important compound for LIBs, can be synthesised from  $\text{Li}_2\text{CO}_3$ ,<sup>24</sup> with research ongoing to convert LiCl directly to LiOH.<sup>25</sup>

The rising demand of LIBs has triggered a growing interest and a focus in quantifying the environmental burdens with the raw material production throughout its life cycle. Ellingsen (2014)<sup>26</sup> established a transparent LIBs LCI on primary data. With regard to lithium production in that research, it is a generalised black box model. Kallitsis *et al.* (2020)<sup>27</sup> studied the LCA of LIBs production in China. This model was based on the model of Ellingsen (2014)<sup>26</sup> and is also a black box model for lithium production. However, the actual environmental impacts of lithium production are expected to be influenced by the specifics of the region and particularly the specific lithium raw material. For example, given the energy intensity of the processes involved, the environmental impact of producing  $\text{Li}_2\text{CO}_3$  or LiOH from spodumene should have a significantly greater environmental impact than if it were from brine. Although previous research<sup>28</sup> suggested that the environmental impacts of  $\text{Li}_2\text{CO}_3$  production was negligible compared to the total transportation impacts caused by an EV, possibly in another continent, they are certainly not negligible for the location where raw material production occurs. Moreover, the rapidly growing demand for lithium(i) raw material over the last decade warrants prudence. This work presents a detailed unit process level model that has been developed as a necessary tool to establish a more reliable and accurate environmental impact assessment of lithium(i) production processes.

Stamp (2012)<sup>28</sup> established a detailed LCI model for  $\text{Li}_2\text{CO}_3$  production by allocating the inputs of  $\text{Li}_2\text{CO}_3$  production according to economics, which increased the accuracy of LCA analysis. However, the primary data used in the research appears to be outdated, and the water balance was neglected. The reliance on assumptions of evaporation may contribute to an inaccurate evaporation efficiency. Kelly (2021)<sup>29</sup> reported a detailed LCI of  $\text{Li}_2\text{CO}_3$  production from brine, but the electrical energy used in the analysis was assumed to be derived from the average Chilean electrical grid fuel mix, overlooking the fact that the national Chilean electrical grid contains different regional grids with distinct fuel mixes. The composition of the regional electrical grid varies according to different climatic characteristics across the nation. For instance, the northern region has abundant solar and wind energy resources. However, coal-fired power plants are also located predominantly in the central and northern regions of Chile.<sup>30</sup> Chordia (2022)<sup>31</sup> updated the life cycle environmental impacts of lithium from brine. Their LCI covered several publications, technical

reports, and Ecoinvent database, but it only offers inputs and outputs without explaining sufficiently the calculation procedures used, nor do they account for the electrical grid mix. Furthermore, the freshwater resources were considered to be extracted from underground aquifers instead of lake-sourced fresh water which is reported in the literature. In contrast, the research results reported here accounts for the separation of minerals from brines and allows for a better understanding of water footprint throughout the process. Khakmardan *et al.* (2023)<sup>32</sup> reported LCA results of different lithium(i) production processes from a global perspective and compared the environmental impacts of lithium production processes from different sources, including brine (Chile), spodumene (Australia and China), hectorite (Mexico), and zinnwaldite (Germany). Lithium(i) production from Chilean brine had the lowest GWP and minimal water consumption, due primarily to the less energy-intensive nature of the brine production process, which involves only pumping the brine to solar evaporation ponds and concentrating it progressively by solar radiation. In contrast, the production of lithium(i) from hard rock sources requires energy-intensive processes such as crushing, grinding, desliming, and flotation, as well as leaching processes and the use of soda ash, sodium hydroxide, and sulfuric acids, which significantly increase water consumption. However, the detailed LCI data of this study<sup>32</sup> is not available for verification. Moreover, the lack of high-quality publicly available data has led to high uncertainty in the results reported.

WF and WSF are increasingly important considerations in the LCA analysis, especially when considering operations taking place in extremely arid regions. Despite the general awareness around this topic, there is still a conceptual debate as to whether including brine water in water footprint analysis is appropriate. Some literature considers only freshwater consumption and excludes brine water from the scope of water consumption due to the unsuitability of brines for direct agricultural or domestic use,<sup>29,31–33</sup> while other literature considers it as the extraction of brine is not accounted for in the depletion of abiotic resources, where extraction of rock minerals extraction impacts are accounted for.<sup>34</sup> In addition, the water scarcity characterisation factors of different regions can also influence the results. In arid regions, the regional water scarcity characterisation factors will be higher than those of other non-arid regions, thereby reflecting in the overall water scarcity impact.<sup>35</sup> Therefore, it is crucial to specify details and relevant parameters in both WF and WSF analysis.

This study addresses the environmental impacts and water consumption of producing battery-grade  $\text{Li}_2\text{CO}_3$  from lithium-containing brine. For this, detailed LCI modelling of the processes used to extract lithium from resources at Salar de Atacama, Chile, was conducted based on state-of-art literature, technical reports, and Ecoinvent database version 3.9.1.<sup>36</sup> The electrical grid mix of the northern Chile region was modelled. Aspen Plus V11 (ref. 37) was used to simulate the production process of  $\text{Li}_2\text{CO}_3$ , including the recycling of input materials. Furthermore, evaporation modelling and water balance were conducted, followed by WF and WSF analysis. The LCA modelling was conducted within the Sphera software.<sup>38</sup> Based



on the ReCiPe 2016 v1.1 Midpoint characterisation method, 13 relevant environmental impacts were analysed and their primary contributions are discussed.

## 2 Methods

### 2.1 Life cycle assessment methodology

Following the ISO standard,<sup>39</sup> a detailed LCI analysis and life cycle assessments were developed to analyse the production of  $\text{Li}_2\text{CO}_3$ .

**2.1.1 Goal and scope.** The functional unit was set as the production of 1 kg of  $\text{Li}_2\text{CO}_3$  of 99.5% purity. The geographical boundary was restricted to Chile, including material inputs, manufacturing processes, transportation, electrical grid mix and other relevant factors. The system boundary was from cradle-to-gate, which includes mining and pumping of brine, evaporation processes, transportation, and chemical manufacturing in a local plant.

**2.1.2 Life cycle inventory analysis.** The LCI of  $\text{Li}_2\text{CO}_3$  production from brine was modelled, having identified the detailed chemical production process, with specific environment and technical parameters from the literature, technical reports and the Ecoinvent database 3.9.1.<sup>33,40,41</sup>

Calculations for material inputs and outputs were based on stoichiometries with the necessary adjustments required to account for the incompleteness of chemical reactions. Subsequently, the production process was simulated using Aspen Plus V11.<sup>37</sup> In addition, the economic allocation approach was applied to  $\text{Li}_2\text{CO}_3$  production of material and energy inputs according to ISO 14040,<sup>39</sup> as there are by-products such as potassium sulphate that are also produced during evaporation their market prices collected from up to date company reports are used as economic allocation factors.<sup>41</sup> Infrastructure construction was not considered in this study due to data unavailability, and considering that this is amortised over the economic materials production during the whole life of the facilities.

The process routes of  $\text{Li}_2\text{CO}_3$  production from Atacama brine are given in Fig. 2. Firstly, underground brine is pumped from the subsurface at the Salar de Atacama core region and deposited into a series of large open-air evaporation ponds to evaporate by solar energy to preconcentrate lithium(I). The common order of precipitation includes halite ( $\text{NaCl}$ ), sylvite ( $\text{KCl}$ ), sylvinit ( $\text{KCl}$  and  $\text{NaCl}$ ), magnesium salts and small quantities of other alkali salts.<sup>42</sup> In order to account for the evaporation process impacts, simulation and calculations using estimation, theoretical calculations based on the Penman equation,<sup>43</sup> and reported measurement data from an on-site meteorological station<sup>44</sup> were used. Detailed explanations of evaporation modelling are provided in subsequent sections. In the Atacama Desert region, freshwater is reported to be extracted from 4 groundwater wells from beneath the foothills of the eastern mountains of the desert.<sup>41</sup> After lithium chloride has reached the drying-up point, at a concentration of approximately 6000 ppm,<sup>17</sup> the concentrated brine is trucked 230 km from desert core to a chemical plant, and is then processed to remove impurities. Treatments include acidification, solvent extraction, re-extraction, precipitation and drying. Borates are removed by acidification and solvent extraction. Re-extraction is used for recycling the organic solvent.  $\text{Mg}^{\text{II}}$  and  $\text{Ca}^{\text{II}}$  are removed by precipitation with soda ash and lime milk. Solid and liquid wastes are collected in surface impoundments. The final concentrated brine is treated with soda ash, thereby precipitating the  $\text{Li}_2\text{CO}_3$  product. After washing, drying, and packaging,  $\text{Li}_2\text{CO}_3$  product is obtained. Water is used primarily for cleaning pipes at the salar evaporation ponds and as wash water in the production process at the plant. Additionally, water is used for preparing solutions, e.g. of  $\text{Na}_2\text{CO}_3$ . Electrical energy is used mainly for operating machinery and equipment such as pumps, filters, reactors, dryers, as well as for powering various facilities within the production process, which relies primarily on energy supplied by the electrical grid and fossil fuels. For the electrical grid fuel mix, the SING (Sistema Interconectado del Norte Grande) electrical grid in northern Chile region was chosen for modelling.<sup>30,45</sup>

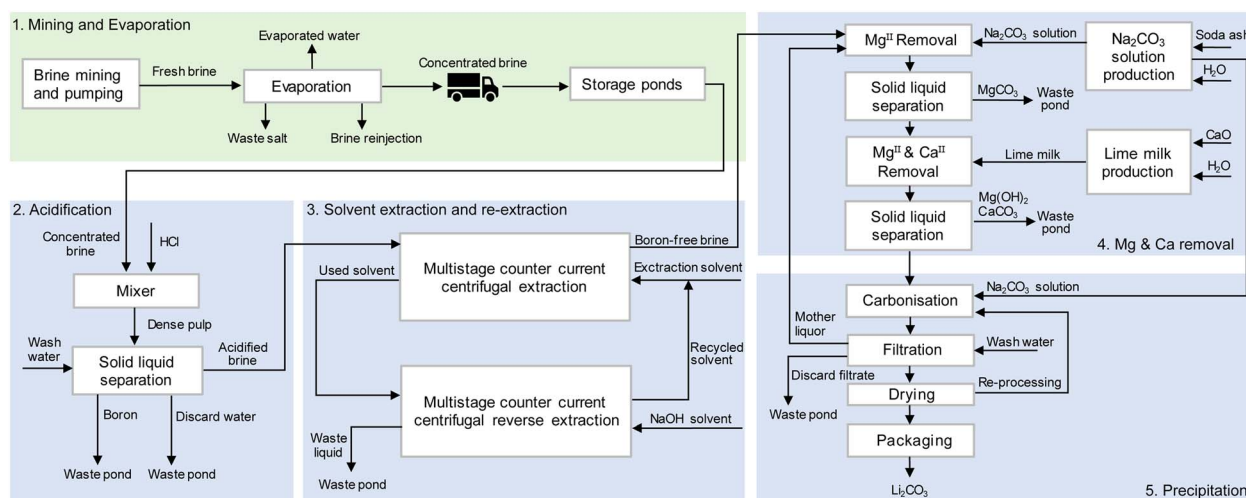


Fig. 2 Lithium carbonate production process flow.





The process modelling was carried out for  $\text{Li}_2\text{CO}_3$  production in the chemical plant using Aspen Plus V11.<sup>37</sup> A heat exchange network was constructed together with the process. The modelling method was set as ELECNRTL. The life cycle inventory was optimised by iteration with Aspen modelling results.

**2.1.3 Life cycle impact assessment.** In order to evaluate the environmental impact of  $\text{Li}_2\text{CO}_3$  product from brine, LCA modelling was conducted using Sphera software.<sup>38</sup> The background processes were retrieved from the Ecoinvent database 3.9.1.<sup>36</sup> The ReCiPe 2016 v1.1 Midpoint characterisation method and the partly regionalised WSF based on AWARE method<sup>35</sup> were used for analysis.

## 2.2 Weather conditions and evaporation modelling

**2.2.1 Weather conditions at Salar de Atacama.** Lithium(I) production from brine is determined mainly by its composition, volume, accessibility, and suitability for local processing.<sup>9</sup> In the Atacama Desert, the climatic conditions are suitable for implementation of a relatively simple evaporation technology. The weather data used here were collected from meteorological stations operated by SQM at the Atacama Desert core,<sup>44</sup> together with regional data from the meteorological directorate of Chile.<sup>46</sup> The monthly precipitation rate and temperature in the Atacama Desert is shown in Fig. 3.

The weather in the Atacama Desert is extremely arid. The average annual precipitation is around  $20 \text{ mm a}^{-1}$ , and the annual precipitation rate of the core region is less than  $10 \text{ mm a}^{-1}$ .<sup>44</sup> The precipitation has seasonal variations; the summer months from February to April have a relatively high level of precipitation which reached  $2.1 \text{ mm}$  in 2023, while there is no precipitation during May to December. The total annual precipitation rate at the Atacama core region is  $7.4 \text{ mm a}^{-1}$ . As shown in Fig. 3, the average daily temperatures typically peak at approximately  $18.9^\circ\text{C}$  and reach a minimum of around  $8.32^\circ\text{C}$  in June. Diurnal temperature fluctuations match this seasonal variability, with maximum and minimum daily temperatures typically separated by around  $14^\circ\text{C}$ .<sup>46</sup> During October to March, winds blow predominantly from the west, and during autumn

and winter, the wind direction is more variable. Morning wind speeds throughout the year are generally  $<2 \text{ m s}^{-1}$ , and wind speeds typically increase in the afternoon, reaching up to  $15 \text{ m s}^{-1}$ .<sup>47</sup> The low precipitation and high solar insolation make this place favourable for evaporation technology. Overall, producing lithium from brine at arid region is cost-effective.

Although solar evaporation is an inexpensive technology as solar energy is readily available in the Atacama Desert region, there are still some disadvantages. The evaporative precipitation steps are slow, normally taking between 8 and 12 months,<sup>41</sup> and may take even 24 months from the pumping process.<sup>17,48</sup> Besides, water evaporated from brine, cannot be recovered economically and may cause a series of hydrological and environmental issues.

**2.2.2 Evaporation modelling.** Three methods were used to simulate the evaporation process. Firstly, it was assumed that up to 95% of brine water needed to be evaporated.<sup>49</sup> In the second approach, the evaporation rate was calculated using the simplified Penman equation.<sup>43</sup> Thirdly, evaporation data measured by class A pan of the on-site meteorological station near the evaporation ponds<sup>44</sup> was used. It is important to note that the evaporation rate of brine can be influenced by weather and salinity severely reducing evaporation rates, so corrections are necessary.<sup>50–53</sup>

The simplified versions of Penman's equations is:<sup>43</sup>

$$E_{\text{PEN}} \approx 0.051(1 - \alpha)R_s\sqrt{T + 9.5} - 2.4\left(\frac{R_s}{R_A}\right)^2 + 0.052(T + 20)\left(1 - \frac{\text{RH}}{100}\right)(a_U - 0.38 + 0.54u) \quad (1)$$

where

$$R_s = R_A\left(0.5 + 0.25\frac{n}{N}\right) \quad (2)$$

$$N \approx 4\varnothing \sin(0.53i - 1.65) + 12 \quad (3)$$

$$R_A \approx 3N \sin(0.131N - 0.95\varnothing) \text{ for } |\varnothing| > \frac{23.5\pi}{180} \quad (4)$$

$E_{\text{PEN}}$  represents the evaporation rate in  $\text{mm day}^{-1}$  calculated from equations  $\alpha$  represents the albedo, of value 0.08 for open water surfaces;  $R_s$  the solar irradiance in  $\text{MJ m}^{-2} \text{ day}^{-1}$ .  $E_{\text{PEN}}$  can be calculated, if  $R_A$ , the extraterrestrial irradiance ( $\text{MJ m}^{-2} \text{ day}^{-1}$ ),  $n$ , the bright sunshine hours ( $\text{h d}^{-1}$ ), and  $N$ , the maximum possible duration of daylight (h) are known.  $T$  represents the average temperature ( $^\circ\text{C}$ ) and RH the relative humidity (%);  $a_U$  equals 1 when original  $N$  can be calculated if  $\varnothing$ , the latitude of the site in radians, which is negative for south, and  $i$ , the rank of month are known. For temperate zones where  $|\varnothing| > \frac{23.5\pi}{180}$ ,  $R_A$  can be calculated if direct data is not available.

The corrected evaporation rate,  $E_O$  ( $\text{mm d}^{-1}$ ) is given by:<sup>54</sup>

$$E_O = K_e K_s E_t \quad (5)$$

where  $E_t$  represents the recorded evaporation in the class A pan or calculations in  $\text{mm day}^{-1}$ ;  $K_e$  is a dimensionless correction factor, the pond coefficient which equals 0.7. This coefficient is

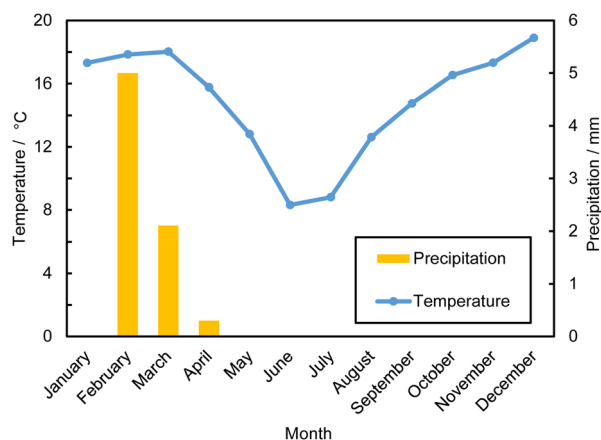


Fig. 3 Monthly precipitation rates and temperatures at Atacama Desert in 2023.<sup>44,46</sup>



related to weather and was estimated in the United States, which has similar weather conditions to those that occur at the Atacama Desert region.  $K_s$  is the salinity reduction coefficient, which also is a dimensionless correction factor and related to liquid average density, which can be determined by the method outlined in IDE (1978).<sup>55</sup>

## 2.3 Water

**2.3.1 Water balance.** Both brine and fresh water are utilised during the brine extraction processes. Up to 95% of the water content in the brine is lost during evaporation, resulting in a concentrated lithium(i)-containing brine. Whether the brine is considered a water resource is still a controversial issue, which brings questions to water balance research.

Brines, which are neither suitable for human use nor for irrigation, are designated as minerals rather than water resources.<sup>56</sup> However, plants and animals that inhabit the Atacama region depend on this water resource, including protected species such as flamingos. Changes in flamingo populations can strongly reflect the extent of environmental damage. Andean and James' flamingos, which are the most threatened species in the Salar de Atacama, declined by approximately 12% and 10% in recent years.<sup>57</sup> Studies have shown a strong correlation between lithium mining activities and local environmental degradation in Atacama.<sup>57,58</sup> However, the direct impact of lithium(i) extraction on the environment and hydrology of the Atacama region has not been stated with certainty.

In this research, minerals and water in the brine are suggested to be considered separately to investigate the water balance of the system. Water contained in the brine is considered as water resource for water balance calculations.<sup>33</sup> Calculating the water balance provides a clearer understanding of the amount of water that needs to be added and the amount of water flowing out of the system. Eqn (6) shows the mass balance of the inputs and outputs in a unit process.<sup>59</sup>

$$W_{ei} + W_{ii} + S_i = W_o + S_o + W_w + W_r \quad (6)$$

where,  $W_{ei}$  represents the external water input;  $W_{ii}$  the internal water input;  $S_i$  the solid input;  $W_o$  the water output;  $S_o$  the solid output;  $W_w$  the wastewater and  $W_r$  the recycled water, as shown in Fig. 4.

**2.3.2 Water footprint and water scarcity.** The WF is divided into three categories:<sup>60</sup> the blue WF which is the consumption of surface and ground water; the green WF is the consumption of precipitation; the grey WF is the consumption of freshwater used to dilute pollutants. Although precipitation is very low, green water and blue water were considered in this study. The

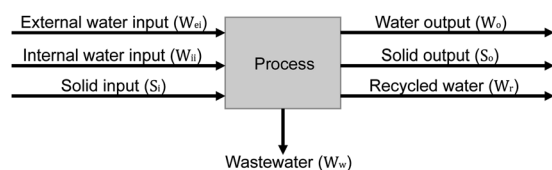


Fig. 4 Water mass balance in an individual unit process.

blue water includes the water incorporated in final products, evaporation, and discharge of used water. Besides, the consumption includes direct consumption and embodied water consumption, which is the WF of materials used in process. Water consumption in the notional  $\text{Li}_2\text{CO}_3$  plant was estimated based on water balance studies. In addition, the WSF can be analysed to provide a more comprehensive understanding and to compare results of the impact of the production on water resources in a specific region. The water scarcity characterisation factor is determined here using the AWARE method, defined for Chile as  $81.38 \text{ m}^3 \text{ world equivalent m}^{-3}$ .<sup>35</sup>

## 2.4 Waste management

During the evaporation production process, a significant amount of salt waste and used brine are generated. The salt waste is typically accumulated near the evaporation ponds on open ground,<sup>41</sup> while used brine is reinjected into the subsurface.<sup>61</sup> However, to the best of our knowledge, there are no reported precise operational details or real case studies of reinjection of large volumes of spent brine. The question whether reinjecting brine may cause dilution of lithium resources, change the ecosystem, or disrupt the stratigraphic structure in Atacama still remains a controversial and unresolved issue.<sup>17</sup> Considering the aforementioned conditions, detailed reinjection analysis is not within the scope of this research. Similarly, during the  $\text{Li}_2\text{CO}_3$  production in the chemical plant, the process generates solid and liquid waste. The composition of liquid waste comprises water with boron(III), organics and some mother liquor containing impurities, while the solid wastes are magnesium carbonate pulp, magnesium hydroxide pulp and calcium carbonate pulp which are generated by precipitation processes. The industrial wastes are disposed in impoundments.<sup>41</sup>

Traditional LCA studies typically neglect the influence of waste management units. However, studying the impact of waste management units is necessary in an arid location like the Atacama Desert where rare animals are present. This study aimed to investigate whether current waste management methods have an impact on the infiltration of groundwater and brine and assess the rational of current waste management practices. The waste management units considered include waste salt piles and surface impoundments.

**2.4.1 Life cycle model for waste salt piles.** Waste piles are facilities where waste is placed for disposal as shown in Fig. 5. However, the leachate from landfills may have negative effects on the groundwater in the surrounding area.

The waste pile was modelled as a rectangular prism model with rainfall as input and leachate as output. The precipitate can be stored in the system, drained laterally, or evaporated back into the atmosphere, as there is little plant cover in the Atacama production region, the plant evapotranspiration was not considered. As the precipitation and temperature fluctuate with seasons, the quantity of water that is infiltrating was calculated using the principle of annual water balance, according to the following eqn (7):



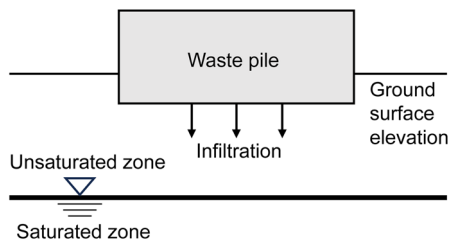


Fig. 5 Waste pile structure illustration.

$$I_a = P_a - E_a - (FC - W) \times T_a \quad (7)$$

where,  $I_a$  represents the annual water infiltration ( $\text{mm a}^{-1}$ ),  $P_a$  represents the annual precipitation in ( $\text{mm a}^{-1}$ ),  $E_a$  represents the annual evaporation ( $\text{mm a}^{-1}$ ),  $FC$  the field capacity ( $\text{vol vol}^{-1}$ ),  $W$  represents the initial water content of the fresh waste ( $\text{vol vol}^{-1}$ ),  $T_a$  represents the thickness of the fresh waste layer accumulated ( $\text{mm a}^{-1}$ ).

**2.4.2 Life cycle model for surface impoundments.** There are three options of configuration of surface impoundment considered here: unlined, single liner and composite liner as

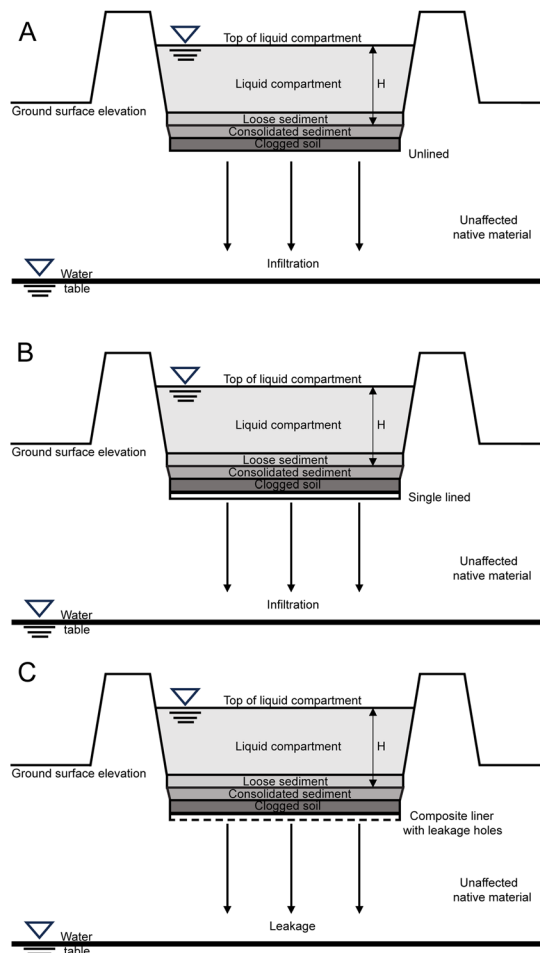


Fig. 6 Three types of surface impoundments considered. (A) Unlined. (B) Single lined. (C) Composite liner with leakage holes.<sup>62</sup>

shown in Fig. 6. The equations and illustrations of the average infiltration rate of the unlined and single lined scenarios are respectively shown in eqn (8) and (9), while for the case of composite liner, the leakage rate was calculated from eqn (10).<sup>62</sup>

$$I = \frac{H_p + D_{fc} + D_{clog}}{\frac{D_{fc}}{K_{fc}} + \frac{D_{clog}}{K_{clog}}} \quad (8)$$

$$I = \frac{H_p + D_{fc} + D_{liner}}{\frac{D_{fc}}{K_{fc}} + \frac{D_{liner}}{K_{liner}}} \quad (9)$$

$$Q = 0.21a^{0.1}h^{0.9}K_s^{0.74}\rho S \quad (10)$$

where  $I$  represents the average infiltration rate ( $\text{m s}^{-1}$ ),  $H_p$  represents the pond depth of wastewater in the surface impoundment (m),  $D_{fc}$  represents the thickness of consolidated sediment layer (m),  $D_{clog}$  and  $D_{liner}$  represent the thickness of clogged soil layer and consolidated sediment layer respectively, which is typically 0.5 m,  $K_{fc}$  represents the saturated hydraulic conductivity of consolidated sediment ( $\text{m s}^{-1}$ ),  $K_{clog}$  and  $K_{liner}$  represent the saturated hydraulic conductivities of clogged soil and liner respectively ( $\text{m s}^{-1}$ ). For the equation for a composite liner,  $Q$  represents the steady-state rate of leakage through holes in the composite liner ( $\text{m}^3 \text{s}^{-1}$ ),  $a$  represents the area of holes in the geomembrane ( $\text{m}^2$ ),  $h$  represents the head of liquid on top of geomembrane (m),  $K_s$  represents the hydraulic conductivity of the low-permeability soil underlying the geomembrane ( $\text{m s}^{-1}$ ),  $\rho$  represents the leak density (holes  $\text{m}^{-2}$ ) and  $S$  represents the footprint of the surface impoundment ( $\text{m}^2$ ). The required parameters can be obtained from USEPA (2003).<sup>63</sup>

## 3 Results and discussion

### 3.1 Life cycle inventory (LCI) analysis

The following sections provide a detailed analysis of the LCI results for  $\text{Li}_2\text{CO}_3$  production from the Atacama Desert brine, starting with the process modelling.

**3.1.1 Process modelling.** The  $\text{Li}_2\text{CO}_3$  production simulation results provide quantified inputs and outputs at the unit process level. After solar evaporation, the concentrated brine is transferred to the chemical plant in which it is acidified with hydrochloric acid, followed by filtration to remove insoluble borates formed with divalent cations (e.g.  $\text{CaB}_4\text{O}_7 \cdot 6\text{H}_2\text{O}$ ), then soluble boron(III) species are extracted by organic solvents in a multistage counter-current centrifugal extraction process. The boron(III) species in the reacted organic solvent is then re-extracted into aqueous NaOH, requiring 6.72 kg NaOH per kg of  $\text{Li}_2\text{CO}_3$  product. The then boron(III)-free brine is reacted with  $\text{Na}_2\text{CO}_3$  to precipitate and recover part of the  $\text{Mg}^{\text{II}}$  as  $\text{MgCO}_3$ , followed by  $\text{Mg}^{\text{II}}$  and  $\text{Ca}^{\text{II}}$  removal as carbonates using lime water, which is cheaper than  $\text{Na}_2\text{CO}_3$  solution. Finally, the purified brine is reacted with  $\text{Na}_2\text{CO}_3$  to precipitate  $\text{Li}_2\text{CO}_3$ , recovered by filtration, then washed with cold water and dried at  $150^\circ\text{C}$  for 3 hours to obtain the final battery-grade product. The mother liquor generated during the precipitation process can



be used to dilute boron-free brine, thereby decreasing the loss of lithium(I) during  $\text{Mg}^{\text{II}}$  and  $\text{Ca}^{\text{II}}$  precipitation.

The simulation results showed that for the chemical plant to produce 1 kg of  $\text{Li}_2\text{CO}_3$ , it required 3.28 kg concentrated brine, and 0.13 kg, 2.79 kg and 10.71 kg of hydrochloric acid, organic solvent, and hydrocarbon diluent, respectively. Precipitation of  $\text{Mg}^{\text{II}}$  and  $\text{Ca}^{\text{II}}$  impurities and carbonisation of the lithium(I) product required 5.79 kg  $\text{Na}_2\text{CO}_3$  in aqueous solution, together with 0.014 kg of lime water. The Aspen modelling of the  $\text{Li}_2\text{CO}_3$  production process validated the LCI inputs and the outputs; finally, discrepancies between modelled results and calculated and collected LCI data inputs were optimised by modelling.

**3.1.2 Evaporation modelling.** Previous publications on LCI on the  $\text{Li}_2\text{CO}_3$  production process appear to have overlooked evaporation rate modelling, which was investigated here by correction and comparison of assumptions, theoretical calculations and measured results. The assumption generally made by previous researchers,<sup>17,49</sup> that up to 95% of the brine is evaporated, resulted in a corrected brine evaporation rate of  $2.71 \text{ mm day}^{-1}$ . The Chilean company Sociedad Química y Minera (SQM) has reported measured brine evaporation rates of  $3.24 \text{ mm day}^{-1}$ , using a metal class A evaporation pan at its measurement stations on site in the Atacama region. The corrected evaporation rate of brine calculated using Penman's eqn (1) was  $2.62 \text{ mm day}^{-1}$ . The estimated result based on earlier authors is similar to that, but significantly lower than that measured by the class A pan, possibly because the side of the pan was also exposed to sunlight, potentially leading to an overestimation of the evaporation rate.<sup>64</sup> Additionally, the liquid placed in the pan for testing was not specified sufficiently, so it is uncertain whether it is brine, groundwater, or some other water. For the theoretical calculation, a simplified version of Penman's equation was used, acknowledging that the wind speed may have a significant effect on the evaporation rate. The evaporation modelling results were used to devise three scenarios in the water balance analysis, as explained in Section 3.2.2.

**3.1.3 Electrical grid fuel mix.** As shown in Fig. 7, the main fuels of the SING electrical grid mix in 2023 were 48.46% natural gas and 34.80% hard coal, accounting for 83.26% of the total

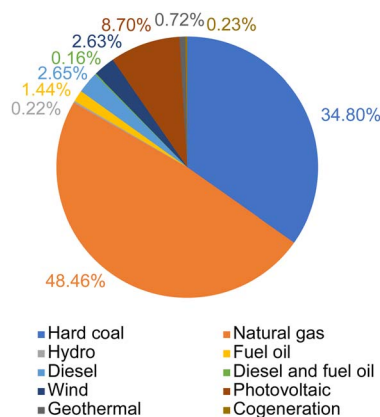


Fig. 7 Northern Chilean electrical grid fuel mix.<sup>45</sup>

electrical grid mix, to which 8.7% was added from photovoltaic energy sources, due to the abundant solar energy resources in the northern Chile region. Hydropower, diesel, fuel, geothermal and cogeneration contributed less to the SING electrical grid fuel mix. Although this specification is very carbon intensive, it is expected that the percentage of coal based power will decrease with time due to the stated intentions in the Chilean government's energy policy, aiming to decommission coal-fired power plants and increase the utilisation of solar power.<sup>30</sup>

**3.1.4 Waste management.** The average water infiltration can be calculated by eqn (7)–(10). Evidently, the climate in the Atacama desert is extremely arid, as the measured annual precipitation is  $7.4 \text{ mm year}^{-1}$ , while the measured evaporation is  $3246.9 \text{ mm year}^{-1}$ .<sup>44</sup> The value of  $T_a$  in eqn (7) cannot be obtained, but the maximum height of waste piles is 30 m.<sup>41</sup> Although the exact values of FC and W were not available, assuming a value of 1 for FC and 0 for W, it can still be estimated that the predicted infiltration will be less than zero. This indicates that there is hardly liquid infiltration from the waste piles formed into the lower layers. Therefore, the infiltration of waste salt from piles will likely have minimal effect on groundwater quality. Similarly, for the infiltration analysis of surface impoundments, whether unlined, single lined or composite lined, the infiltration rate and leakage are extremely small. As a result of the range of values for parameters  $K_{fc}$  and  $a$ , for the unlined model, the average infiltration rate was predicted to range from  $2.24 \times 10^{-7} \text{ m s}^{-1}$  to  $3.07 \times 10^{-7} \text{ m s}^{-1}$ ; for the single lined model, the infiltration rate ranged from  $1.94 \times 10^{-8} \text{ m s}^{-1}$  to  $1.98 \times 10^{-8} \text{ m s}^{-1}$ ; for the composite liner model, the leakage rate ranged from  $4.83 \times 10^{-8} \text{ m s}^{-1}$  to  $6.09 \times 10^{-8} \text{ m s}^{-1}$ . Consequently, infiltration may have little influence on underground water and brine. Therefore, it is inferred that rainwater management or a collection system may not be needed.

While the effect of waste infiltration may be negligible, the waste produced during evaporation and accumulated near the evaporation ponds occupies significant land area. Based on calculations, the annual production of  $1.8 \times 10^5 \text{ t a}^{-1}$  of  $\text{Li}_2\text{CO}_3$  will generate  $1.43 \times 10^7 \text{ t a}^{-1}$  of waste salts, consisting mainly of sodium and potassium salts. As assumed by Flexer (2018),<sup>17</sup> the salt mixture was considered to have an average volumetric density of  $2 \text{ kg dm}^{-3}$ . As a result, this will produce waste with a volume of  $7.16 \times 10^6 \text{ m}^3 \text{ a}^{-1}$ . Assuming that each waste pile has a height of 30 m,<sup>41</sup> the total required area is  $2.39 \times 10^5 \text{ m}^2 \text{ a}^{-1}$  which is expected to expand with increasing annual production, requiring timely implementation of waste disposal.

## 3.2 Life cycle impact assessment analysis

**3.2.1 Life cycle impact assessment.** A cradle-to-gate LCA for producing 1 kg of  $\text{Li}_2\text{CO}_3$  from brine was conducted based on the optimised LCI produced. Fig. 8 presents the thirteen different environmental impacts assigned to different key contributing processes.

Among all impact categories, use of NaOH and sodium carbonate, water supply, and electrical energy supply were the most significant contributors, with minor additional





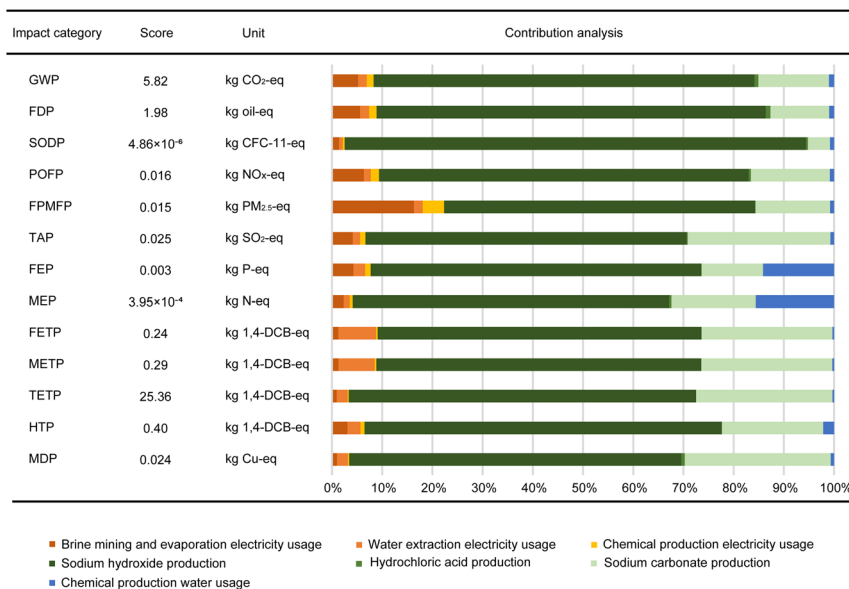


Fig. 8 Environmental impacts of lithium carbonate production at the Atacama Desert, disaggregated to key contributing processes.

contributions from other sources. This arose mainly from the NaOH requirement in the re-extraction process of borates from organic to aqueous solvents. The high mass-specific electrical energy requirement of the chlor-alkali electrolytic process for NaOH production was the dominant contributor. Additionally, Na<sub>2</sub>CO<sub>3</sub>, used for Mg<sup>II</sup> and Ca<sup>II</sup> removal and for precipitation of the Li<sub>2</sub>CO<sub>3</sub> product, led to environmental impacts. The entire production process requires electrical energy from the grid and water for solution preparation and as wash water, which also causes significant burdens.

Despite the high CO<sub>2</sub> footprint of NaOH production being included in the analysis, as shown in Table 1, the overall GWP of the Li<sub>2</sub>CO<sub>3</sub> production was predicted as 5.82 kg CO<sub>2</sub> (kg Li<sub>2</sub>CO<sub>3</sub>)<sup>-1</sup>, driven primarily by use of NaOH (75.84%), Na<sub>2</sub>CO<sub>3</sub> (14.01%) and electrical energy (8.30%). If the re-extraction process was not included in the production process, the overall GWP was predicted to decrease to 1.41 kg CO<sub>2</sub> (kg Li<sub>2</sub>CO<sub>3</sub>)<sup>-1</sup>. However, this would result in increased costs and large volumes

of waste organic solvents to be treated. The major environmental impacts contributors are summarised in Table 1. NaOH, Na<sub>2</sub>CO<sub>3</sub>, electrical energy and water use were the dominant contributors to fossil depletion potential (FDP), stratospheric ozone depletion (SODP), photochemical ozone formation, human health (POFP), terrestrial acidification (TAP), freshwater ecotoxicity (FETP), marine ecotoxicity (METP), terrestrial ecotoxicity (TETP), human toxicity, cancer (HTP) and metal depletion (MDP). For fine particulate matter formation potential (FPMFP), electrical energy was the second largest contributor, accounting for 18.08%. For freshwater eutrophication (FEP) and marine eutrophication (MEP), water use contributed 14.15% and 15.60%, respectively, as did Na<sub>2</sub>CO<sub>3</sub> (12.23% and 16.80%, respectively).

Fig. 8 reports a predicted GWP of 5.82 kg CO<sub>2</sub> (kg Li<sub>2</sub>CO<sub>3</sub>)<sup>-1</sup> produced from brine, whereas previously research reported different GWP values shown in Table 2.<sup>28,29,31,32</sup> However, it is important to note that previous results were predicted using simplistic unit process approaches without detailed theoretical calculations and modelling, such as of evaporation. It is unclear whether those authors considered the effects of boron(III) re-extraction processes; they did not include effects of regional electrical energy simulations, and used data across different years, so a range of GWP values are justified.

Table 1 Major environmental impact contributors for Li<sub>2</sub>CO<sub>3</sub> production

| Impact | Major contributions   |
|--------|---|
| GWP    | NaOH (75.84%), Na <sub>2</sub> CO <sub>3</sub> (14.01%), electricity (8.30%)  |
| FDP    | NaOH (77.56%), Na <sub>2</sub> CO <sub>3</sub> (11.67%)                       |
| SODP   | NaOH (91.89%), Na <sub>2</sub> CO <sub>3</sub> (4.37%)                        |
| POFP   | NaOH (73.64%), Na <sub>2</sub> CO <sub>3</sub> (15.71%)                       |
| FPMFP  | NaOH (61.90%), electricity (18.08%), Na <sub>2</sub> CO <sub>3</sub> (14.83%) |
| TAP    | NaOH (63.97%), Na <sub>2</sub> CO <sub>3</sub> (28.40%)                       |
| FEP    | NaOH (65.89%), Na <sub>2</sub> CO <sub>3</sub> (12.23%), water (14.15%)       |
| MEP    | NaOH (63.02%), Na <sub>2</sub> CO <sub>3</sub> (16.80%), water (15.60%)       |
| FETP   | NaOH (64.49%), Na <sub>2</sub> CO <sub>3</sub> (26.05%)                       |
| METP   | NaOH (64.71%), Na <sub>2</sub> CO <sub>3</sub> (26.10%)                       |
| TETP   | NaOH (69.14%), Na <sub>2</sub> CO <sub>3</sub> (27.14%)                       |
| HTP    | NaOH (71.16%), Na <sub>2</sub> CO <sub>3</sub> (20.17%), water (2.17%)        |
| MDP    | NaOH (66.13%), Na <sub>2</sub> CO <sub>3</sub> (29.06%)                       |

Table 2 Comparisons of GWP results for Li<sub>2</sub>CO<sub>3</sub> production from brine with previously reported results

| Study year | GWP/kg CO <sub>2</sub> (kg Li <sub>2</sub> CO <sub>3</sub> ) <sup>-1</sup> | Reference  |
|------------|--|------------|
| 2012       | 2.02   | 28         |
| 2021       | 2.9  | 29         |
| 2022       | 3.5  | 31         |
| 2023       | 4–5  | 32         |
| 2024       | 5.82   | This study |



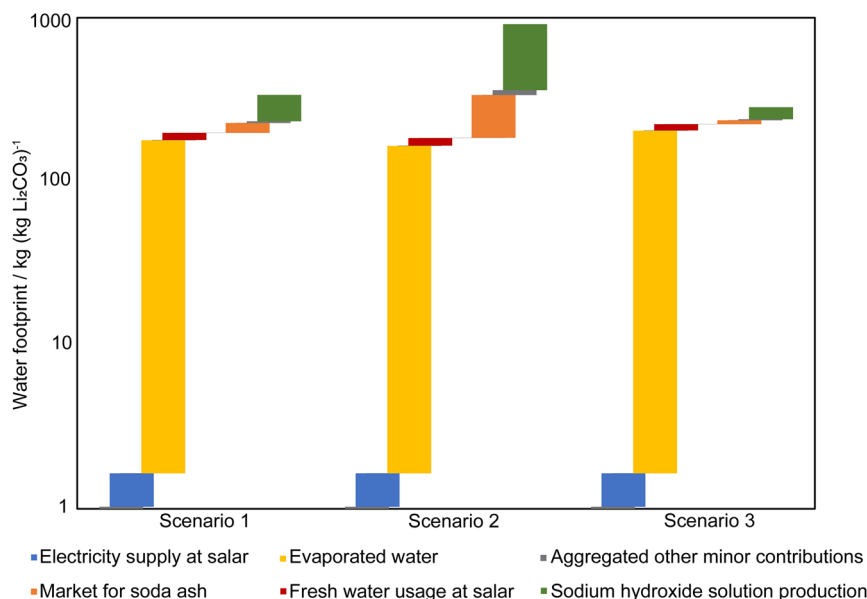


Fig. 9 Water footprint components for lithium carbonate production in the Atacama Desert.

**3.2.2 Water footprint (WF) and water scarcity footprint (WSF).** Water balance analyses were used to calculate water footprints and water scarcity footprints reported in Fig. 9. The blue WF was predicted for three different evaporation modelling scenarios, with a production period of one year; the green WF was negligible due to the limited precipitation. The minor contributors to water footprint were aggregated and detailed information can be found in the ESI.†

For the assumed evaporation scenario 1, the total was 160 kg (kg Li<sub>2</sub>CO<sub>3</sub>)<sup>-1</sup> without considering water evaporation from brine, and the blue WF of the chemical plant production process blue WF accounted for 87.50% of the total. The NaOH production process consumed a significant amount of water, accounting for 74.83% of the total blue WF of the chemical plant production process. Excluding the NaOH production process, the total blue WF for all other processes was 55.41 kg (kg Li<sub>2</sub>CO<sub>3</sub>)<sup>-1</sup>. If water evaporation from brine was considered as a consumption of underground water resources, the blue WF was predicted to increase by 175.8 kg (kg Li<sub>2</sub>CO<sub>3</sub>)<sup>-1</sup>.

For scenario 2, using Penman's eqn (1), the total blue WF was predicted as 749 kg (kg Li<sub>2</sub>CO<sub>3</sub>)<sup>-1</sup> without considering water evaporation from brine, since decreased evaporation rates led to increased volumes of concentrated brine supplied to the chemical plant. According to the calculations, the quantity of chemicals added was proportional to the brine volume, which increased the overall water footprint. Therefore, the first process of brine evaporation is crucial as it influences the inputs to the chemical plant and water consumption, thereby affecting production processes and costs. Similarly, if water evaporation from brine was considered, the blue WF would increase by 164 kg (kg Li<sub>2</sub>CO<sub>3</sub>)<sup>-1</sup>.

For scenario 3, the measured evaporation rate scenario, according to calculations, the blue WF consumption was 80 kg (kg Li<sub>2</sub>CO<sub>3</sub>)<sup>-1</sup> without considering water evaporation from

brine, with 75.14% attributed to the chemical plant production and 24.86% to the mining and evaporation processes. The actual amount of brine available for evaporation, calculated from the total annual brine extraction was 179.7 kg (kg Li<sub>2</sub>CO<sub>3</sub>)<sup>-1</sup>. However, due to the higher evaporation rate, there was an excessive water evaporation from brine; the amount of evaporated water should be 202.6 kg (kg Li<sub>2</sub>CO<sub>3</sub>)<sup>-1</sup>, which is 12.73% more than the actual value.

Fig. 10 shows the WSF for Li<sub>2</sub>CO<sub>3</sub> production from brine in Chile. The 2023 AWARE water scarcity index for Chile is 81.38 m<sub>world eq.</sub><sup>3</sup> (kg Li<sub>2</sub>CO<sub>3</sub>)<sup>-1</sup>.<sup>35</sup> The WSFs were calculated taking water evaporation from brine into account for the three scenarios: 27.45 m<sub>world eq.</sub><sup>3</sup> (kg Li<sub>2</sub>CO<sub>3</sub>)<sup>-1</sup> for scenario 1, 74.55 m<sub>world eq.</sub><sup>3</sup> (kg Li<sub>2</sub>CO<sub>3</sub>)<sup>-1</sup> for scenario 2 and 23.12 m<sub>world eq.</sub><sup>3</sup> (kg Li<sub>2</sub>CO<sub>3</sub>)<sup>-1</sup> for scenario 3. The water scarcity effects of the Atacama Desert arise primarily from water evaporation from brine and direct utilisation of freshwater at the processing plant. If

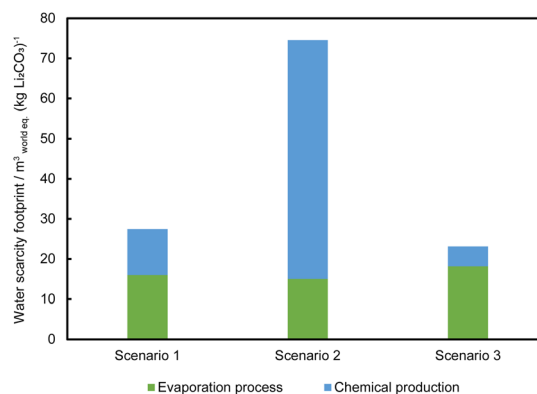


Fig. 10 Water scarcity footprint results for three scenarios: scenario 1 for an assumed evaporation rate; scenario 2 for Penman's equation; scenario 3 using measured evaporation rates with the class A pan.



the prior brine evaporation concentration process is sufficient, the water demand for the processing plant would be relatively reasonable.

Some reports argue that the impact of brine extraction should not be included in water balance analyses, but should be evaluated through the hydrogeology analysis of the salt flats.<sup>58,65,66</sup> However, the extracted brine, through the evaporation process, results in concentrated brine and takes part in the overall water balance of the system. Therefore, we suggested that it should be considered within the complete scope of water analysis. Furthermore, the extremely high water scarcity factor of Chile indicates the need for cautious water resource consumption in arid regions, especially in the Atacama Desert where the WSF may be even higher than the national average. It is essential to decrease water use and increase water recycling. However, presently, the evaporated brine which should be considered as a resource as well, as it exits the system and cannot be recovered by conventional evaporation methods. The development of new technology avoiding water evaporation from brine and reducing the amount of chemical usage will greatly benefit the arid region by reducing its water scarcity effect.

**3.2.3 Sensitivity analysis.** The Chilean electrical grid fuel mix and variations in brine concentration were identified as critical parameters for sensitivity analysis. These factors were analysed to evaluate their effects on the overall environmental impacts. Between 2030 and 2050, Chile's electrical grid fuel mix is predicted to undergo significant changes to form a more sustainable energy future, driven by a strong shift towards renewable energy sources. As shown in Table 3, the share of wind and photovoltaic energy will increase significantly. Concentrated solar power and battery energy storage will also grow.

Conversely, there will be a decrease in reliance on fossil fuels, hydropower, biomass, and geothermal energy; coal will be phased out entirely.<sup>67</sup>

Table 3 presents the expected Chilean electrical grid fuel mix evolution in the near- (2030) and longer-term future (2050).<sup>67</sup> Fig. 11 presents the respective sensitivity analysis results comparing the base case with each of these two scenarios. The transition to increasingly renewable energy-dominated grid

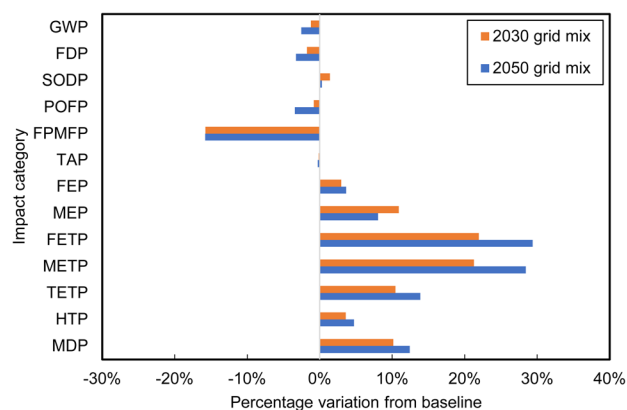


Fig. 11 Changes in life cycle impact scores of lithium carbonate production from Atacama brines due to expected electrical grid evolution.

mixes in Chile by 2030 and 2050 results in significant environmental benefits, as compared to the present base case, including decreases in GWP, FDP, POFP, FPMFP and TAP up to 16%. However, the energy shift also introduces new challenges. SODP, FEP, MEP, FETP, METP, TETP, HTP and MDP are expected to increase by up to 30%, due to the renewable energy infrastructure specifics, such as the need for battery energy storage systems, solar panels, and wind turbines. Due to high  $\text{Li}^{\text{I}}$  concentrations in Atacama brines, specific energy consumptions of solar evaporation processes are low.<sup>68</sup> Therefore, switching to clean energy sources has minimal effect on decreasing GWP (1.22% and 2.54%).

For the sensitivity analysis of brine concentration, it was assumed that the ratios of ion concentrations in brines remained constant, while brine concentrations were diluted by 25% and 50%, reflecting the exploitation of lower quality resources formed by geological and hydrological processes that remained unchanged. The compositions of the diluted brines considered are presented in Table 4.

Fig. 12 presents results of the sensitivity analysis for the two brine dilution scenarios, which were predicted to cause increases in overall environmental impacts, with life cycle impact scores increasing further as concentrations decreased. Specifically, a 25% decrease in brine concentration led to

Table 3 Chile electrical grid fuel mix in 2030 and 2050 (ref. 67)

| Energy type                   | Contribution/% |       |
|-------------------------------|----------------|-------|
|                               | 2030           | 2050  |
| Battery energy storage system | 2.32           | 3.17  |
| Diesel                        | 4.08           | 0.57  |
| Wind                          | 24.07          | 33.52 |
| Photovoltaic                  | 26.89          | 36.13 |
| Concentrated solar power      | 13.64          | 17.22 |
| Liquified natural gas         | 6.15           | 0.93  |
| Hydro                         | 20.09          | 7.30  |
| Biomass                       | 2.20           | 0.97  |
| Geothermal                    | 0.53           | 0.19  |
| Coal                          | —              | —     |

Table 4 Brine compositions for scenarios assuming decreased concentrations of ions in brine by 25% and 50%

| Composition             | Base case/wt% | 25% reduction/wt% | 50% reduction/wt% |
|-------------------------|---------------|-------------------|-------------------|
| $\text{Li}^{\text{I}}$  | 0.15          | 0.11              | 0.08              |
| $\text{Cl}^{\text{I}}$  | 16.04         | 12.03             | 8.02              |
| $\text{Na}^{\text{I}}$  | 7.60          | 5.70              | 3.80              |
| $\text{K}^{\text{I}}$   | 1.85          | 1.39              | 0.93              |
| $\text{Ca}^{\text{II}}$ | 0.03          | 0.02              | 0.015             |
| $\text{Mg}^{\text{II}}$ | 0.96          | 0.72              | 0.48              |
| $\text{SO}_4^{2-}$      | 1.65          | 1.24              | 0.83              |
| $\text{B}^{\text{III}}$ | 0.06          | 0.05              | 0.03              |
| $\text{H}_2\text{O}$    | 71.66         | 78.75             | 85.83             |



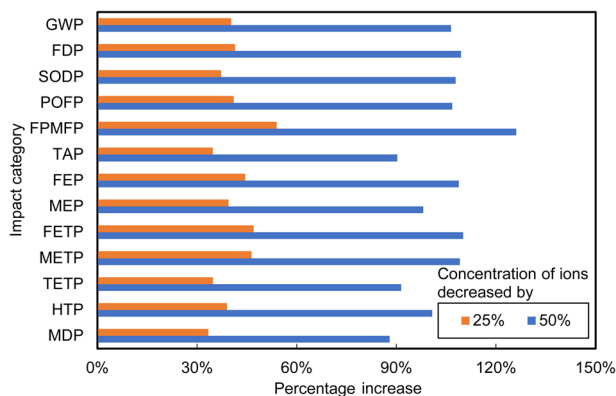


Fig. 12 Changes in life cycle impact of lithium carbonate production from Atacama brines due to 25% and 50% dilution of ion concentrations.

increases in life cycle environmental impacts ranging from 33% to 54%, whereas a 50% reduction in brine concentration caused life cycle impacts to increase by 88% to 126% across the various categories. These increases were due primarily to lower brine concentrations necessitating the processing of larger volumes of brine to produce 1 kg of  $\text{Li}_2\text{CO}_3$ , in turn intensifying requirements for chemicals and energy. Consequently, overall life cycle environmental impacts increased significantly.

### 3.3 Process improvements and alternative methods

Improvement of the present process requires optimisation of removal processes of boron(III) and other impurities. Firstly, boron(III) removal was predicted to be the primary source of pollution, mostly due to NaOH production. Replacing the hydrogen evolution/water reduction reaction ( $2\text{H}_2\text{O} + 2\text{e}^- \rightarrow \text{H}_2 + 2\text{OH}^-$ ) at cathodes in conventional chlor-alkali membrane electrolyzers with the oxygen-reduction reaction ( $\text{O}_2 + 2\text{H}_2\text{O} + 4\text{e}^- \rightarrow 4\text{OH}^-$ ) at oxygen depolarised cathodes (ODC) could decrease of electrical energy usage by *ca.* 25%, thereby decreasing  $\text{CO}_2$  emissions and GWPs.<sup>69</sup> Presently, ODC technology offers the most environmentally sustainable method of chlor-alkali production.<sup>70,71</sup> Furthermore, molar ratios of  $\text{H}_2\text{O}$  consumed to  $\text{OH}^-$  ions produced in conventional membrane chlor-alkali processes are *ca.* 1, whereas that ratio is 0.5 for oxygen reduction cathodes, so enabling decreased water consumption.

Despite decades of operation of the boron(III) solvent extraction process, ongoing research is exploring alternative methods such as nanofiltration, to remove boron(III) from brine. However, nanofiltration is 1.4 to 1.7 times more polluting than solvent extraction because of its greater consumption of electrical energy.<sup>72</sup> In addition, the use of environmentally benign solvents and improved extraction and re-extraction techniques has the potential to decrease the consumption of input materials so decreasing environmental burdens.

Secondly, companies and academics are researching new technologies intensively to recover lithium(I) from brines, since lithium(I) recoveries are <50% by solar evaporation. The new

techniques, such as solvent extraction, adsorption, nanofiltration, and electrochemical methods, aim to increase  $\text{Li}^+$  production rates without relying on evaporation. In the extraction of lithium(I), solvent extraction offers 75% to 99% greater recovery rates.<sup>73–77</sup> However, large scale production would require large volumes of organic solvent, challenging its recovery and suitable equipment selection.<sup>21</sup> Alternatively, lithium(I) extraction by adsorption would be a simple and attractive technique due to high lithium(I) selectivity (92–99%) and adsorption capacity.<sup>78–80</sup> However, this technique in large-scale production can result in blockage of the ion channels reducing adsorbing capacity.<sup>21</sup> Additionally, the adsorbents may need frequent replacement making implementation complicated and potentially expensive. Nanofiltration for lithium(I) extraction is a simple method that can be conducted at room temperature, but lithium(I) recoveries have been reported to be relatively low, ranging from 12% to 55%.<sup>81–83</sup> Electrochemical methods for lithium(I) extraction offer great potential, avoiding the need for boron(III) removal processes and have low water ( $1.1$  to  $47.5 \text{ dm}^3 \text{ s}^{-1}$ ) and electrical energy consumptions ( $0.001$  to  $0.013 \text{ kW h per mol Li}^+$ ).<sup>84</sup> Additionally, production times have been decreased to days and even hours. For example, lithium(I) in brine can be recovered selectively by electrochemical deintercalation/intercalation system ( $\text{LiFePO}_4/\text{FePO}_4$  EDI system), during which the  $\text{Mg}^{2+}$ ,  $\text{Ca}^{2+}$ ,  $\text{SO}_4^{2-}$  and  $\text{B}_4\text{O}_7^{2-}$  removal rates were above 94%.<sup>85</sup> In addition,  $\text{LiMn}_2\text{O}_4/\text{Li}_{1-x}\text{Mn}_2\text{O}_4$  (LMO) electrochemical systems with porous electrodes is also a promising method, which can recover lithium(I) directly from brine at a high rate and low specific electrical energy consumptions.<sup>86</sup>

Overall, all those methods mentioned above offer distinct advantages and challenges in lithium(I) extraction, highlighting the necessity for comprehensive evaluation and consideration of factors such as recovery efficiency, environmental impact, operational feasibility, and cost benefit analysis in large-scale production scenarios.

### 3.4 Limitations and future perspectives

Although a detailed LCA of  $\text{Li}_2\text{CO}_3$  production has been developed, it still has some limitations and shortcomings. Specifically, the waste management model was simplified; rectangular cuboid units were employed based on the methods of USEPA,<sup>62</sup> whereas waste piles often have conical or trapezoidal shapes in reality. These differences can affect the thickness of the accumulated fresh waste layer and further influence infiltration rates. Therefore, a more careful evaluation of the model parameters for real cases is required for an in-depth investigation of waste management. For water scarcity analysis, the water scarcity factor used is the Chilean average value. However, it is essential to obtain the latest water scarcity factor specific to the production site at the core of the Atacama Desert for a more detailed analysis at the regional level.

In recent years, several coal-fired power stations have been decommissioned in Chile and replaced with solar and wind energy generation. This change is expected to make the future electrical grid mix in Chile cleaner, and less carbon intensive.





Therefore, it is reasonable to explore the environmental impact of Chile energy transition on lithium(i) production in the future. A comprehensive LCA study can be conducted of alternative methods of lithium(i) extraction from brine to compare with conventional evaporative techniques. This analysis can help to evaluate the environmental impacts, water resource consumption, production output, duration, and economic benefits of each method, providing comprehensive guidance for lithium(i) production.

## 4 Conclusions

An up-to-date and more detailed LCI model has been established, based on chemical stoichiometry calculations, parameter modelling, and existing literature, technical reports, and the Ecoinvent database. This model involved optimisation through simulations, as well as calculations for every step of the process, including recycling. Due to the varying regional characteristics of brine production in each salar, and distinct freshwater resources surrounding different brine extraction sites, investigation of individual salars characteristics and extraction processes is considered necessary. Simulations of the northern Chile electricity grid mix, still dominated by fossil fuels, has helped produce more accurate results that are regionally specific. For waste management, although the accumulation of waste generated during Li carbonate production may not have had a significant impact on infiltration, still it is shown to result in occupation of significant land areas.

Detailed and complete analysis of thirteen life cycle environmental impacts of this Li<sup>i</sup> extraction process has predicted relatively low GWP (5.82 kg CO<sub>2</sub> (kg Li<sub>2</sub>CO<sub>3</sub>)<sup>-1</sup>) and other impacts, but relatively high TETP (24.57 kg 1,4-DB eq. (kg Li<sub>2</sub>CO<sub>3</sub>)<sup>-1</sup>) due to NaOH production. Considering water issues, three scenarios for the evaporation process have been simulated, adjusted, and compared to analyse the water balance results. Although the water footprint of the process was shown not to have been significant (0.29 m<sup>3</sup> (kg Li<sub>2</sub>CO<sub>3</sub>)<sup>-1</sup> to 0.92 m<sup>3</sup> (kg Li<sub>2</sub>CO<sub>3</sub>)<sup>-1</sup>), it is crucial to note that this water has been extracted and pumped from an underground resource that is scarce in an extremely arid region. Therefore, the WSF of this seemingly low water-consuming Li<sup>i</sup> production process was predicted to be relatively high significant (23.12 m<sub>world equiv.</sub><sup>3</sup> (kg Li<sub>2</sub>CO<sub>3</sub>)<sup>-1</sup> to 74.55 m<sub>world equiv.</sub><sup>3</sup> (kg Li<sub>2</sub>CO<sub>3</sub>)<sup>-1</sup>). In addition to those disadvantages, the time-consuming production also resulted in low predicted lithium(i) recoveries and recovery rates during the evaporation process.

The rapidly growing demand in the Li<sub>2</sub>CO<sub>3</sub> market is encouraging the conception and development of novel lithium(i) recovery processes. Although many alternative solutions have been studied and even up-scaled, they have not specifically addressed the question of how the brine will be treated after lithium(i) recovery. Through our water balance analysis, a significant volume of water from brines was predicted to be lost from the system by evaporation; in such an extremely arid area those losses should not be ignored but considered as a potential resource for recovery. The results provided important insights of the life cycle impacts of Li<sub>2</sub>CO<sub>3</sub> production and

associated industries and can help guide lithium(i) production activities. Additionally, the results offer a scientific basis for environmental management in arid and similar regions.

## Abbreviations

|       |  |
|-------|--|
| EDI   | Electrochemical Deintercalation/Intercalation                                      |
| FDP   | Fossil Depletion Potential   |
| FEP   | Freshwater Eutrophication Potential  |
| FETP  | Freshwater Ecotoxicity Potential   |
| FPMFP | Fine Particulate Matter Formation Potential  |
| GWP   | Global Warming Potential   |
| HTP   | Human Toxicity Potential, cancer   |
| LCA   | Life Cycle Assessment  |
| LCI   | Life Cycle Inventory   |
| LIB   | Lithium-Ion Battery  |
| LMO   | LiMn <sub>2</sub> O <sub>4</sub> /Li <sub>1-x</sub> Mn <sub>2</sub> O <sub>4</sub> |
| MDP   | Metal Depletion Potential  |
| MEP   | Marine Eutrophication Potential  |
| METP  | Marine Ecotoxicity Potential   |
| POFP  | Photochemical Oxidant Formation Potential, human health                            |
| SING  | Sistema Interconectado del Norte Grande  |
| SODP  | Stratospheric Ozone Depletion Potential  |
| SQM   | Sociedad Química y Minera  |
| TAP   | Terrestrial Acidification Potential  |
| TETP  | Terrestrial Ecotoxicity Potential  |
| WF    | Water Footprint  |
| WSF   | Water Scarcity Footprint   |

## List of symbol definitions and units

|                    |  |
|--------------------|--|
| $\alpha$           | Albedo (/1)  |
| $a$                | Area of holes in the geomembrane (m <sup>2</sup> )                                   |
| $a_U$              | Wind function coefficient (/1)   |
| $D_{\text{clog}}$  | Thickness of clogged soil layer (m)  |
| $D_{\text{fc}}$    | Thickness of consolidated sediment layer (m)   |
| $D_{\text{liner}}$ | Thickness of consolidated sediment layer (m)   |
| $E_a$              | Annual evaporation (mm a <sup>-1</sup> )   |
| $E_o$              | Corrected evaporation rate (mm day <sup>-1</sup> )                                   |
| $E_{\text{PEN}}$   | Calculated evaporation rate using Penman equation (mm day <sup>-1</sup> )            |
| $E_t$              | Recorded evaporation rate in the class A pan or calculations (mm day <sup>-1</sup> ) |
| FC                 | Field capacity (vol vol <sup>-1</sup> )  |
| $h$                | Head of liquid on top of geomembrane (m)   |
| $H_p$              | Pond depth of wastewater in the surface impoundment (m)                              |
| $i$                | Rank of month (/1)   |
| $I$                | Average infiltration rate (m s <sup>-1</sup> )                                       |
| $I_a$              | Annual water infiltration (mm a <sup>-1</sup> )                                      |
| $K_{\text{clog}}$  | Saturated hydraulic conductivity of clogged soil (m s <sup>-1</sup> )                |
| $K_{\text{fc}}$    | Saturated hydraulic conductivity of consolidated sediment (m s <sup>-1</sup> )       |
| $K_{\text{liner}}$ | Saturated hydraulic conductivity of liner (m s <sup>-1</sup> )                       |
| $K_e$              | Pond coefficient (/1)  |



|          |  |
|----------|--|
| $K_s$    | Hydraulic conductivity of the low-permeability soil underlying the geomembrane ( $\text{m s}^{-1}$ ) |
| $K_s$    | Salinity reduction coefficient (1)   |
| $n$      | Bright sunshine hours per day (h)  |
| $N$      | Maximum possible daylight duration (h)   |
| $P_a$    | Annual precipitation ( $\text{mm a}^{-1}$ )  |
| $Q$      | Steady-state rate of leakage through holes in composite liner ( $\text{m}^3 \text{s}^{-1}$ )         |
| RH       | Relative humidity (%)  |
| $R_A$    | Extraterrestrial irradiance ( $\text{MJ m}^{-2} \text{day}^{-1}$ )                                   |
| $R_s$    | Solar irradiance ( $\text{MJ m}^{-2} \text{day}^{-1}$ )  |
| $S$      | Footprint of the surface impoundment ( $\text{m}^2$ )  |
| $S_i$    | Solid input ( $\text{kg (kg Li}_2\text{CO}_3)^{-1}$ )  |
| $S_o$    | Solid output ( $\text{kg (kg Li}_2\text{CO}_3)^{-1}$ )   |
| $T$      | Average temperature ( $^{\circ}\text{C}$ )   |
| $T_a$    | Thickness of the fresh waste layer accumulated ( $\text{mm a}^{-1}$ )                                |
| $u$      | Wind speed ( $\text{m s}^{-1}$ )   |
| $W$      | Initial water content of the fresh waste ( $\text{vol vol}^{-1}$ )                                   |
| $W_{ei}$ | External water input ( $\text{kg (kg Li}_2\text{CO}_3)^{-1}$ )                                       |
| $W_{ii}$ | Internal water input ( $\text{kg (kg Li}_2\text{CO}_3)^{-1}$ )                                       |
| $W_o$    | Water output ( $\text{kg (kg Li}_2\text{CO}_3)^{-1}$ )   |
| $W_r$    | Recycled water ( $\text{kg (kg Li}_2\text{CO}_3)^{-1}$ )   |
| $W_w$    | Wastewater ( $\text{kg (kg Li}_2\text{CO}_3)^{-1}$ )   |
| $\phi$   | Latitude of the site (Rad)   |
| $\rho$   | Leak density (holes $\text{m}^{-2}$ )  |

## Data availability

The data supporting this article have been included as part of the ESI.†

## Author contributions

Zijing He: conceptualisation, methodology, software, investigation, formal analysis, writing – original draft. Anna Korre: conceptualisation, supervision, methodology, writing – review & editing. Geoff Kelsall: supervision, writing – review & editing. Zhenggang Nie: methodology. Melanie Colet: methodology, input data.

## Conflicts of interest

There are no conflicts to declare.

## Acknowledgements

The research reported is part of an Imperial College London PhD research scholarship for the lead author, supplemented by Anne Seagrim Accommodation Scholarship.

## References

- 1 U.S. Geological Survey, *Mineral Commodity Summaries 2024*, 2024.
- 2 International Energy Agency, Net Zero Roadmap: A Global Pathway to Keep the 1.5  $^{\circ}\text{C}$  Goal in Reach, 2023.
- 3 International Energy Agency, Global EV Outlook 2023, <https://www.iea.org/reports/global-ev-outlook-2023/executive-summary>, (accessed 1 April 2024).
- 4 B. W. Jaskula, *2018 Minerals Yearbook Lithium [Advance Release]*, U.S. Department of the Interior, U.S. Geological Survey, 2020.
- 5 H. Vikström, S. Davidsson and M. Höök, *Appl. Energy*, 2013, **110**, 252–266.
- 6 C. Grosjean, P. H. Miranda, M. Perrin and P. Poggi, *Renewable Sustainable Energy Rev.*, 2012, **16**, 1735–1744.
- 7 M. E. Q. Pilson, *An Introduction to the Chemistry of the Sea*, Cambridge University Press, 2012.
- 8 A. Shahmansouri, J. Min, L. Jin and C. Bellona, *J. Cleaner Prod.*, 2015, **100**, 4–16.
- 9 S. E. Kesler, P. W. Gruber, P. A. Medina, G. A. Keoleian, M. P. Everson and T. J. Wallington, *Ore Geol. Rev.*, 2012, **48**, 55–69.
- 10 A. Seip, S. Safari, D. M. Pickup, A. V. Chadwick, S. Ramos, C. A. Velasco, J. M. Cerrato and D. S. Alessi, *Chem. Eng. J.*, 2021, **426**, 130713.
- 11 A. Kumar, H. Fukuda, T. A. Hatton and J. H. V. Lienhard, *ACS Energy Lett.*, 2019, **4**, 1471–1474.
- 12 M. Figueira, D. Rodríguez-Jiménez, J. López, M. Reig, J. L. Cortina and C. Valderrama, *Desalination*, 2023, **549**, 116321.
- 13 S. Kim, J. Kim, S. Kim, J. Lee and J. Yoon, *Environ. Sci.: Water Res. Technol.*, 2018, **4**, 175–182.
- 14 V. Devda, K. Chaudhary, S. Varjani, B. Pathak, A. K. Patel, R. R. Singhanian, M. J. Taherzadeh, H. H. Ngo, J. W. C. Wong, W. Guo and P. Chaturvedi, *Bioengineered*, 2021, **12**, 4697–4718.
- 15 N. A. A. Qasem, R. H. Mohammed and D. U. Lawal, *npj Clean Water*, 2021, **4**, 1–15.
- 16 A. Siekierka, M. Bryjak, A. Razmjou, W. Kujawski, A. N. Nikoloski and L. F. Dumée, *Membranes*, 2022, **12**, 343.
- 17 V. Flexer, C. F. Baspineiro and C. I. Galli, *Sci. Total Environ.*, 2018, **639**, 1188–1204.
- 18 B. Swain, *Sep. Purif. Technol.*, 2017, **172**, 388–403.
- 19 L. Talens Peiró, G. Villalba Méndez and R. U. Ayres, *JOM*, 2013, **65**, 986–996.
- 20 D. E. Garrett, *Handbook of Lithium and Natural Calcium Chloride*, 2004.
- 21 J. F. Song, L. D. Nghiem, X.-M. Li and T. He, *Environ. Sci.: Water Res. Technol.*, 2017, **3**, 593–597.
- 22 C. Shi, Y. Jing and Y. Jia, *J. Mol. Liq.*, 2016, **215**, 640–646.
- 23 R. N. Hader, R. L. Nielsen and M. G. Herre, *Ind. Eng. Chem.*, 1951, **43**, 2636–2646.
- 24 M. Grágeda, A. González, W. Alavia and S. Ushak, *Energy*, 2015, **89**, 667–677.
- 25 V. T. Nguyen, C. Deferm, W. Caytan, S. Riaño, P. T. Jones and K. Binnemans, *J. Sustainable Metall.*, 2023, **9**, 107–122.
- 26 L. A.-W. Ellingsen, G. Majeau-Bettez, B. Singh, A. K. Srivastava, L. O. Valøen and A. H. Strømman, *J. Ind. Ecol.*, 2014, **18**, 113–124.
- 27 E. Kallitsis, A. Korre, G. Kelsall, M. Kupfersberger and Z. Nie, *J. Cleaner Prod.*, 2020, **254**, 120067.
- 28 A. Stamp, D. J. Lang and P. A. Wäger, *J. Cleaner Prod.*, 2012, **23**, 104–112.



- 29 J. C. Kelly, M. Wang, Q. Dai and O. Winjobi, *Resour., Conserv. Recycl.*, 2021, **174**, 105762.
- 30 Ministerio de Energía, *Anuario Estadístico de Energía año 2022*, 2020.
- 31 M. Chordia, S. Wickerts, A. Nordelöf and R. Arvidsson, *Resour., Conserv. Recycl.*, 2022, **187**, 106634.
- 32 S. Khakmardan, M. Rolinck, F. Cerdas, C. Herrmann, D. Giurco, R. Crawford and W. Li, *Procedia CIRP*, 2023, **116**, 606–611.
- 33 V. Schenker, C. Oberschelp and S. Pfister, *Resour., Conserv. Recycl.*, 2022, **187**, 106611.
- 34 A. C. Schomberg, S. Bringezu and M. Flörke, *Commun. Earth Environ.*, 2021, **2**, 1–10.
- 35 A.-M. Boulay, J. Bare, L. Benini, M. Berger, M. J. Lathuillière, A. Manzardo, M. Margni, M. Motoshita, M. Núñez, A. V. Pastor, B. Ridoutt, T. Oki, S. Worbe and S. Pfister, *Int. J. Life Cycle Assess.*, 2018, **23**, 368–378.
- 36 Ecoinvent Association, Ecoinvent Database 3.9.1, 2024, <https://ecoinvent.org/>.
- 37 Aspen Tech, Aspen Plus, 2024, <https://www.aspentech.com/en/products/engineering/aspen-plus>.
- 38 Sphera Solutions, Life Cycle Assessment (LCA) Software, 2023, <https://about.sphera.com/ps>.
- 39 The International Organization for Standardization, ISO 14040: 2006a Environmental Management-Life Cycle Assessment-Principles and Framework, 2006.
- 40 I. Wilkomirsky, *US Pat.*, 5993759, 1999.
- 41 Sociedad Química y Minera de Chile, *Technical Report Summary Operation Report Salar de Atacama*, Av. Las Condes 11.700, Vitacura. Santiago, Chile, 2022.
- 42 T. Tran and V. T. Luong, in *Lithium Process Chemistry*, Elsevier, 2015, pp. 81–124.
- 43 J. D. Valiantzas, *J. Hydrol.*, 2006, **331**, 690–702.
- 44 Sociedad Química y Minera de Chile, SQM monitor en línea, <https://www.sqmsenlinea.com/meteorology/232>, accessed 3 April 2024.
- 45 Economic Charge Dispatch Center of the SING, The Chile CDED-SING, [http://cdec2.cdec-sing.cl/pls/portal/cdec.pck\\_web\\_coord\\_elec.sp\\_pagina?p\\_id=5197](http://cdec2.cdec-sing.cl/pls/portal/cdec.pck_web_coord_elec.sp_pagina?p_id=5197), accessed 1 April 2024.
- 46 Dirección General De Aeronáutica Civil and Dirección Meteorológica de Chile, Servicios Climáticos, <https://climatologia.meteochile.gob.cl/application/requerimiento/producto/RE1011>, accessed 3 April 2024.
- 47 S. K. Kampf, S. W. Tyler, C. A. Ortiz, J. F. Muñoz and P. L. Adkins, *J. Hydrol.*, 2005, **310**, 236–252.
- 48 W. Zhu, W. Xu, D. Liu, L. He, X. Liu and Z. Zhao, *Electrochim. Acta*, 2024, **475**, 143519.
- 49 F. Habashi, *Handbook of Extractive Metallurgy*, Wiley-VCH, 1997.
- 50 J. F. Muñoz-Pardo, C. A. Ortiz-Astete, L. Mardones-Pérez and P. de Vidts-Sabelle, *Tecnol. Cienc. Agua*, 2004, **19**, 69–81.
- 51 T. A. Newson and M. Fahey, *Eng. Geol.*, 2003, **70**, 217–233.
- 52 Y. Fujiyasil, *PhD thesis*, The University of Western Australia, 1997.
- 53 T. A. Newson, Y. Fujiyasu and M. Fahey, *Proceedings of the Fourteenth International Conference on Soil Mechanics and Foundation Engineering*, 1997, vol. 3, pp. 1973–1978.
- 54 L. Mardones, *El litio, un nuevo recurso para Chile*, 1986, 181–216.
- 55 F. Ide, *PhD thesis*, Universidad de Chile, 1978.
- 56 Sociedad Química y Minera de Chile, Fresh water and brine: why they are different, <https://www.sustainablelithium.com/what/>, accessed 5 February 2024.
- 57 J. S. Gutiérrez, J. N. Moore, J. P. Donnelly, C. Dorador, J. G. Navedo and N. R. Senner, *Proc. R. Soc. B*, 2022, **289**, 20212388.
- 58 W. Liu, D. B. Agusdinata and S. W. Myint, *Int. J. Appl. Earth Obs. Geoinf.*, 2019, **80**, 145–156.
- 59 J. C. Molinare, *PhD thesis*, Imperial College London, 2014.
- 60 M. M. Aldaya, A. K. Chapagain, A. Y. Hoekstra and M. M. Mekonnen, *The Water Footprint Assessment Manual Setting the Global Standard*, 2012.
- 61 Vicepresidencia Operaciones Potasio Litio, Undécimo Informe de Extracción Anual de Salmuera de las Operaciones en el Salar de Atacama, 2019.
- 62 U.S. Environmental Protection Agency, EPA's Composite Model for Leachate Migration with Transformation Products (EPACMTP) Technical Background Document, 2023.
- 63 U.S. Environmental Protection Agency, EPA's Composite Model for Leachate Migration with Transformation Products (EPACMTP) Parameters/Data Background Document, 2023.
- 64 J. Finch and A. Calver, *Methods for the Quantification of Evaporation from Lakes*, 2008.
- 65 M. A. Marazuela, E. Vázquez-Suñé, C. Ayora and A. García-Gil, *Sci. Total Environ.*, 2020, **703**, 135605.
- 66 W. Liu and D. B. Agusdinata, *Extr. Ind. Soc.*, 2021, **8**, 100927.
- 67 Ministerio de Energía, Proyecciones Eléctricas, <https://energia.gob.cl/pelp/proyecciones-electricas>, accessed 5 August 2024.
- 68 Sociedad Química y Minera de Chile, Sustainability of lithium production in Chile, 2021.
- 69 Global Corporate Website, Saving energy in chlorine production, <https://www.covestro.com/en/sustainability/flagship-solutions/oxygen-depolarized-cathode>, accessed 17 April 2024.
- 70 I. Garcia-Herrero, M. Margallo, R. Onandía, R. Aldaco and A. Irabien, *Sustain. Prod. Consum.*, 2017, **12**, 44–58.
- 71 I. Garcia-Herrero, M. Margallo, R. Onandía, R. Aldaco and A. Irabien, *Sci. Total Environ.*, 2017, **580**, 147–157.
- 72 J. Wu, B. Li and J. Lu, *Clean Technol. Environ. Policy*, 2021, **23**, 1981–1991.
- 73 T. Sekimoto, S. Nishihama and K. Yoshizuka, *Solvent Extr. Res. Dev., Jpn.*, 2018, **25**, 117–123.
- 74 D. Shi, B. Cui, L. Li, X. Peng, L. Zhang and Y. Zhang, *Sep. Purif. Technol.*, 2019, **211**, 303–309.
- 75 L. Zhang, L. Li, D. Shi, X. Peng, F. Song, F. Nie and W. Han, *Hydrometallurgy*, 2018, **175**, 35–42.
- 76 W. Xiang, S. Liang, Z. Zhou, W. Qin and W. Fei, *Hydrometallurgy*, 2017, **171**, 27–32.



- 77 L. Ji, Y. Hu, L. Li, D. Shi, J. Li, F. Nie, F. Song, Z. Zeng, W. Sun and Z. Liu, *Hydrometallurgy*, 2016, **162**, 71–78.
- 78 S. Wang, P. Li, X. Zhang, S. Zheng and Y. Zhang, *Hydrometallurgy*, 2017, **174**, 21–28.
- 79 J.-L. Xiao, S.-Y. Sun, X. Song, P. Li and J.-G. Yu, *Chem. Eng. J.*, 2015, **279**, 659–666.
- 80 X. Shi, D. Zhou, Z. Zhang, L. Yu, H. Xu, B. Chen and X. Yang, *Hydrometallurgy*, 2011, **110**, 99–106.
- 81 Y. Li, Y. Zhao, H. Wang and M. Wang, *Desalination*, 2019, **468**, 114081.
- 82 A. Somrani, A. H. Hamzaoui and M. Pontie, *Desalination*, 2013, **317**, 184–192.
- 83 X. Wen, P. Ma, C. Zhu, Q. He and X. Deng, *Sep. Purif. Technol.*, 2006, **49**, 230–236.
- 84 J. A. A. Dietz, J. T. V. Valero, M. A. C. Lagrille and G. E. M. Naranjo, *Undergraduate thesis*, Universidad de Chile, 2021.
- 85 D. Liu, Z. Zhao, W. Xu, J. Xiong and L. He, *Desalination*, 2021, **519**, 115302.
- 86 D. Liu, W. Xu, J. Xiong, L. He and Z. Zhao, *Sep. Purif. Technol.*, 2021, **270**, 118809.

